Chemistry and Physics of a Molecular-Based Magnet Containing Three Spin Carriers, with a Fully Interlocked Structure

Humberto O. Stumpf,[†,1] Lahcène Ouahab,[‡] Yu Pei,[†] Pierre Bergerat,[†] and Olivier Kahn*[,†]

Contribution from the Laboratoire de Chimie Inorganique, URA No. 420, Université de Paris Sud, 91405 Orsay, France, and the Laboratoire de Chimie du Solide et Inorganique Moléculaire, URA No. 1495, Université de Rennes 1, 35042 Rennes, France

Received December 13, 1993[⊕]

Abstract: The compound of formula $(rad)_2Mn_2[Cu(opba)]_3(DMSO)_2\cdot 2H_2O$ (hereafter abbreviated as $(rad)_2Mn_2Cu_3$) has been synthesized; rad^+ stands for the radical cation 2-(1-methylpyridinium-4-yl)-4,4,5,5-tetramethylimidazoline-1-oxyl 3-oxide, and opba stands for *o*-phenylenebis(oxamato). The crystal structure has been solved (space group, *Cc*; lattice parameters, a = 25.379(3) Å, b = 25.146(3) Å, c = 18.845(6) Å, β = 131.52(4)°, Z = 4) and has revealed quite an unusual architecture. The structure consists of two nearly perpendicular graphite-like networks with edge-sharing hexagons. The corners of each hexagon are occupied by Mn(II) ions, and the middles of the edges by Cu(II) ions. The two networks are interlocked, the center of each hexagon being occupied by a Cu(II) ion belonging to a perpendicular hexagon. $(rad)_2Mn_2Cu_3$ contains three kinds of spin carriers: Mn(II) and Cu(II) ions, antiferromagnetically coupled through oxamato bridges, and rad^+ radical cations, bridging the Cu(II) ions through the nitronyl nitroxide groups and forming rad^+–Cu(II) chains. The magnetic and EPR properties of $(rad)_2Mn_2Cu_3$ have been studied in some detail. The temperature dependence of $\chi_M T$ (χ_M being the molar magnetic susceptibility and T the temperature) shows a minimum around 115 K characteristic of a ferrimagnetic behavior and then a divergence as T approaches the very low temperatures. The temperature dependence of the magnetization has confirmed that a long-range magnetic ordering occurs at T_c = 22.5 K. The field dependence of the magnetization, $M = f(H)$, has been measured at 4.2 K up to 200 kOe. The compound behaves as a soft magnet, with a very weak coercive field. The $M = f(H)$ curve shows an extremely high zero-field susceptibility, as expected for a magnet and then a smooth increase of M as H increases. This behavior has been attributed to the progressive alignment of the rad^+ spins along the field direction. In zero field, the radical cations are antiferromagnetically coupled with the Mn_2Cu_3 metal core, a situation which probably results from ferromagnetic interactions between nearest neighbor spin carriers along the rad^+–Cu(II) chains. The average value of the rad^+–Cu(II) interaction parameter has been estimated from the high-field range of the $M = f(H)$ curve and found as J_{radCu} = 11.5 cm^{-1} ($\mathbf{H} = -J_{radCu}\mathbf{S}_{rad}\cdot\mathbf{S}_{Cu}$). The X-band powder EPR spectra have also been investigated. Above T_c the spectra show a single resonance centered at g = 1.995 at 290 K and at g = 1.955 at 23 K. At T_c new features appear, which are strongly temperature dependent. A qualitative picture of the ferromagnetic resonance in $(rad)_2Mn_2Cu_3$ has been proposed. All the structural and physical data have been discussed, and some perspectives of our findings have been presented.

Introduction

The first molecular-based magnets were described in 1986.[2,3] Since then there has been a rapid development in this field of research,[4] and special programs have been launched both in Europe (in the frame of the European Community) and in Japan.

The various goals along this line may be summarized as follows: (i) First of all, to design new molecular-based compounds exhibiting a spontaneous magnetization below a critical temperature T_c. Quite a few approaches have been utilized. Some groups focus on purely organic magnets;[5-8] some others work with metal-containing magnetic units;[9-15] finally, other groups use both organic radicals and metal ions as spin carriers.[16-24] (ii) For a given family of compounds, to shift T_c toward higher temperatures. This requires increasing the interactions between spin carriers along the three directions of the space. Indeed, the magnetic ordering is most generally a three-dimensional phenomenon. In no case may it occur at one dimension.[25,42-44,57] (iii) Again for a given family of compounds, to increase both the coercive field and the remnant magnetization which confer a memory effect to the magnetic materials. For this purpose it

† Laboratoire de Chimie Inorganique, Université de Paris Sud.
‡ Laboratoire de Chimie du Solide et Inorganique Moléculaire, Université de Rennes 1.
⊕ Abstract published in *Advance ACS Abstracts*, April 1, 1994.
(1) Permanent address: Departamento de Quimica, Universidade Federal de Minas Gerais, CEP 31270, Belo-Horizonte, MG-Brazil.
(2) Miller, J. S.; Calabrese, J. C.; Epstein, A. J.; Bigelow, R. W.; Zhang, J. H.; Reiff, W. M. *J. Chem. Soc., Chem. Commun.* **1986**, 1026.
(3) Pei, Y.; Verdaguer, M.; Kahn, O.; Sletten, J.; Renard, J. P. *J. Am. Chem. Soc.* **1986**, *108*, 7428.
(4) Proceedings of the Symposium on the Chemistry and Physics of Molecular Based Magnetic Materials. Iwamura, H., Miller, J. S., Eds. *Mol. Cryst. Liq. Cryst.* **1993**, *233*.
(5) Turek, P.; Nozawa, K.; Shiomi, D.; Awaga, K.; Inabe, T.; Maruyama, Y.; Kinoshita, M. *Chem. Phys. Lett.* **1991**, *80*, 327.
(6) Nakazawa, Y.; Tamura, M.; Shirakawa, N.; Shiomi, D.; Takahashi, M.; Kinoshita, M.; Ishikawa, M. *Phys. Rev. B* **1992**, *46*, 8906.
(7) Allemand, P. M.; Khemani, K. C.; Koch, A.; Wudl, F.; Holczer, K.; Donovan, S.; Grüner, G.; Thompson, J. D. *Science* **1991**, *253*, 301.
(8) Chiarelli, R.; Nowak, M. A.; Rassat, A.; Tholence, J. L. *Nature* **1993**, *363*, 147.
(9) Kahn, O.; Pei, Y.; Verdaguer, M.; Renard, J. P.; Sletten, J. *J. Am. Chem. Soc.* **1988**, *110*, 782.
(10) Nakatani, K.; Bergerat, P.; Codjovi, E.; Mathoniére, C.; Pei, Y.; Kahn, O. *Inorg. Chem.* **1991**, *30*, 3977.
(11) Nakatani, K.; Carriat, P. Y.; Journaux, Y.; Kahn, O.; Lloret, F.; Renard, J. P.; Pei, Y.; Sletten, J.; Verdaguer, M. *J. Am. Chem. Soc.* **1989**, *111*, 5739.
(12) Tamaki, H.; Zhong, Z. J.; Matsumoto, N.; Kida, S.; Koikawa, M.; Achiwa, N.; Hashimoto, Y.; Okawa, H. *J. Am. Chem. Soc.* **1992**, *114*, 6974.
(13) Pei, Y.; Kahn, O.; Nakatani, K.; Codjovi, E.; Mathoniére, C.; Sletten, J. *J. Am. Chem. Soc.* **1991**, *113*, 6558.
(14) Gadet, V.; Mallah, T.; Castro, I.; Verdaguer, M.; Veillet, P. *J. Am. Chem. Soc.* **1992**, *114*, 9213.
(15) Mallah, T.; Thiebaut, S.; Verdaguer, M.; Veillet, P. *Science* **1993**, *262*, 1554.
(16) Miller, J. S.; Calabrese, J. C.; Rommelmann, H.; Chittipedi, S. R.; Zhang, J. H.; Reiff, W. M.; Epstein, A. J. *J. Am. Chem. Soc.* **1987**, *109*, 769.

0002-7863/94/1516-3866$04.50/0

seems to be necessaryto use spin carriers presenting a large magnetic anisotropy.[26] If it was so, the purely organic magnets would not be good candidates to obtain such a memory effect. (iv) To explore all the other physical properties of the molecular-based magnets, in particular those which are more specific to the molecular state, like the optical properties or the processability.

Our group is involved in all these directions. In the last period, however, our main efforts have concerned the increasing of the dimensionality of the compounds. We first designed Mn(II)-Cu(II) chain compounds;[27] then we adjusted the relative positions of the chains within the crystal lattice in a way that would prevent the antiparallel alignment of the chain spins.[9] Afterward, we attempted to cross-link the chains chemically[28] or to make them closer to each other as a result of thermal treatment.[10] Then, recently, we succeeded in designing two-dimensional magnets of the formula $(cat)_2Mn_2[Cu(opba)]_3 \cdot L$, where cat^+ stands for a cation, L for solvent molecules, and opba for *o*-phenylenebis-(oxamato).[29] $[Cu(opba)]^{2-}$ is the building block:

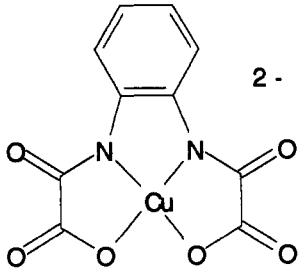

Two compounds of this type have been described, whose formulae are $(NBu_4)_2Mn_2[Cu(opba)]_3 \cdot 6DMSO \cdot H_2O$ (hereafter abbreviated as $(NBu_4)_2Mn_2Cu_3$) and $(NBu_4)_2Mn_2[Cu(opba)]_3$, with DMSO = dimethyl sulfoxide and NBu_4^+ = *N*-tetrabutylammonium. Their magnetic properties are very similar, except that the critical temperature is 15 K for the former and 22 K for the latter.

Our next target was then to connect the layers in order to increase further the dimensionality. Our idea was that using a magnetic cation for cat^+ might result in a magnetic coupling between the layers. For this, we decided to utilize the radical cation 2-(1-methylpyridinium-4-yl)-4,4,5,5-tetramethylimidazoline-1-oxyl 3-oxide (hereafter abbreviated as rad^+)

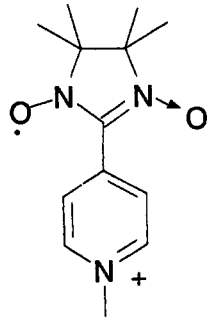

and obtained a compound of formula $(rad)_2Mn_2[Cu(opba)]_3 \cdot (DMSO)_2 \cdot 2H_2O$, hereafter abbreviated as $(rad)_2Mn_2Cu_3$. In this paper, we will describe the synthesis of this compound, its unique crystal structure, and its magnetic and EPR properties. A first communication concerning this compound already appeared.[30]

Experimental Section

Syntheses. The radical cation iodide[31] rad^+I^- and the tetrabutylammonium salt of the copper(II) precursor[29] $(NBu_4)_2[Cu(opba)]$ were prepared as already described. The copper(II) precursor $(rad)_2[Cu(opba)] \cdot H_2O$ was obtained as follows: a solution of 4.22 g (5.3×10^{-3} mol) of $(NBu_4)_2[Cu(opba)]$ in 90 mL of CH_2Cl_2 was added into a solution of 4 g (10.6×10^{-3} mol) of rad^+I^- in 250 mL of CH_2Cl_2. A polycrystalline powder precipitated. After 20 min this precipitate was filtered off, washed with CH_2Cl_2, and dried under vacuum. $(rad)_2[Cu(opba) \cdot H_2O$ is slightly hygroscopic and must be kept in the dark and at low temperature. Anal. Calc for $C_{36}H_{44}N_8O_{11}Cu$: C, 52.20; H, 5.31; N, 13.53; O, 21.25; Cu, 7.67. Found: C, 52.19; H, 5.29; N, 13.50; O, 20.82; Cu, 7.60. $(rad)_2Mn_2[Cu(opba)]_3(DMSO)_2 \cdot 2H_2O$ was synthesized as follows: 0.011 g (5.6×10^{-5} mol) of $MnCl_2 \cdot 4H_2O$ was added into a solution of 0.441 g (3.5×10^{-4} mol) of $(rad)_2[Cu(opba)] \cdot H_2O$ in 25 mL of DMSO. The mixture was stirred at room temperature for 30 min. The color slowly turned to green. The mixture was maintained at room temperature with a water bath, and 25 mL of water was then very slowly added. Afterward, the mixture was poured into a beaker of 10-cm diameter and allowed to stand. The first crystals appeared within a few hours. They were collected after a few days, washed with a 1/1 $DMSO/H_2O$ mixture, and dried in a desiccator. This synthesis is rather delicate but is perfectly reproducible if the experimental conditions are carefully followed and the copper(II) precursor is of high purity. A small change in the experimental conditions may result in chain compounds with MnCu stoichiometry or in other phases with the Mn_2Cu_3 stoichiometry. Anal. Calc for $C_{60}H_{66}N_{12}O_{26}S_2Cu_3Mn_2$: C, 41.52; H, 3.83; N, 9.68; S, 3.69; Cu, 10.98; Mn, 6.33. Found: C, 41.39; H, 4.09; N, 9.41; S, 3.65; Cu, 10.67; Mn, 6.31.

Crystallographic Data Collection and Structure Determination. A green crystal of dimensions $1.0 \times 0.2 \times 0.12$ mm^3 was mounted on an Enraf-Nonius CAD4 diffractometer with graphite-monochromated Mo Kα radiation ($\lambda = 0.710\,73$ Å). The cell dimensions were refined by the least squares method from the setting angles of 25 centered reflections ($8° \leq 2\theta \leq 15°$). The crystal data are summarized in Table SI. The intensities were collected by θ–2θ scans. Three standard reflections were measured every hour and revealed no fluctuations in intensities. One set of reflections was collected up to $2\theta = 46°$. The Lorentz and polarization corrections were applied. The absorption correction was performed using the DIFABS procedure. The extinction conditions suggest the $C2/c$ or Cc space groups. The latter was retained because of the successful solution and refinement of the structure in that group.

The structure was solved by direct method and successive Fourier difference syntheses. The structure was refined by the block cascade full matrix least squares method. The methyl groups of one nitronyl nitroxide radical show high disorder, as observed commonly in other related radicals.[32] The water molecules are distributed on four sites. The disordered DMSO and H_2O molecules were refined with occupancy factors fixed at 0.5. After refinement of positional and anisotropic (β_{ij}) thermal parameters for non-hydrogen atoms, the positions of the H-atoms were calculated [d(C–H) = 0.95 Å; B_{eq} = 5 Å^2] and included as a fixed contribution to F_c. Scattering factors and corrections for anomalous dispersion were taken from ref 33. All the calculations were performed on a MicroVax 3100 computer using the Enraf-Nonius Molen programs.[34]

The bond lengths around the metal ions and some other selected interatomic separations are given in Table 1. Atomic coordinates, bond

(17) Broderick, W. E.; Thompson, J. A.; Day, E. P.; Hoffman, B. M. *Science* **1990**, *249*, 401.
(18) Yee, G. T.; Manriquez, J. M.; Dixon, D. A.; McLean, R. S.; Groski, D. M.; Flippen, R. B.; Naraya, K. S. *Adv. Mater.* **1991**, *3*, 309.
(19) Broderick, W. E.; Hoffman, B. M. *J. Am. Chem. Soc.* **1991**, *113*, 6334.
(20) Eichhorn, D. M.; Skee, D. C.; Broderick, W. E.; Hoffman, B. M. *Inorg. Chem.* **1993**, *32*, 491.
(21) Caneschi, A.; Gatteschi, D.; Renard, J. P.; Rey, P.; Sessoli, R. *Inorg. Chem.* **1989**, *28*, 1976; **1989**, *28*, 3314.
(22) Caneschi, A.; Gatteschi, D.; Sessoli, R.; Rey, P. *Acc. Chem. Res.* **1989**, *22*, 392.
(23) Miller, J. S.; Calabrese, J. C.; McLean, R. S.; Epstein, A. J. *Adv. Mater.* **1992**, *4*, 498.
(24) Manriquez, J. M.; Yee, G. T.; McLean, R. S.; Epstein, A. J.; Miller, J. S. *Science* **1991**, *252*, 1415.
(25) Kahn, O. *Molecular Magnetism*; VCH: New York, 1993.
(26) Stumpf, H. O.; Pei, Y.; Michaut, C.; Kahn, O.; Renard, J. P.; Ouahab, L. *Chem. Mater.*, in press.
(27) Pei, Y.; Verdaguer, M.; Kahn, O.; Sletten, J.; Renard, J. P. *Inorg. Chem.* **1987**, *26*, 138.
(28) Nakatani, K.; Kahn, O.; Mathoniére, C.; Pei, Y.; Zakine, C. *New J. Chem.* **1990**, *14*, 861.
(29) Stumpf, H. O.; Pei, Y.; Kahn, O.; Sletten, J.; Renard, J. P. *J. Am. Chem. Soc.* **1993**, *115*, 6738.
(30) Stumpf, H. O.; Ouahab, L.; Pei, Y.; Grandjean, D.; Kahn, O. *Science* **1993**, *261*, 447.
(31) Awaga, K.; Inabe, T.; Nakamura, T.; Matsumoto, M.; Kawabata, Y.; Maruyama, Y. *Chem. Lett.* **1991**, 1777.
(32) Pei, Y.; Ouahab, L.; le Berre, F.; Tholence, J. L.; Kahn, O. To be published.

Table 1. Selected Bond Lengths and Intermolecular Contacts (Å) for $(rad)_2Mn_2[Cu(opba)]_3(DMSO)_2 \cdot 2H_2O$[a]

	Bond Lengths		
Cu1–N1	1.91 (2)	Mn1–O3	2.27 (2)
Cu1–N2	1.98 (2)	Mn1–O4	2.21 (2)
Cu1–O1	2.06 (1)	Mn1–O9	2.24 (2)
Cu1–O2	2.00 (2)	Mn1–O10	2.22 (2)
Cu2–N3	1.94 (2)	Mn1–O17	2.15 (2)
Cu2–N4	1.93 (2)	Mn1–O18	2.18 (2)
Cu2–O7	1.96 (2)	Mn2–O5	2.20 (2)
Cu2–O8	1.99 (1)	Mn2–O6	2.16 (1)
Cu3–N5	1.95 (3)	Mn2–O11	2.18 (2)
Cu3–N6	1.95 (2)	Mn2–O12	2.23 (1)
Cu3–O13	1.95 (2)	Mn2–O15	2.17 (2)
Cu3–O14	1.95 (2)	Mn2–O16	2.18 (2)
	Intermolecular Contacts		
Cu1–O1S	2.55 (6)	Mn1–O4R	6.55 (3)[i]
Cu1–O2S	2.57 (5)	Mn2–O1R	6.63 (2)[ii]
Cu2–O1R	2.94 (2)[ii]	Mn2–O2R	6.64 (2)[iii]
Cu2–O3R	2.90 (2)	Mn2–O3R	5.35 (3)[iv]
Cu3–O2R	2.82 (1)[ii]	Mn2–O4R	5.31 (3)
Cu3–O4R	3.01 (2)	Mn1–O1R	6.25 (2)[v]
Mn1–O3R	6.54 (2)[vi]	Mn1–O2R	6.03 (2)

[a] Symmetry code: (i) $x - 1/2, 1/2 + y, z$; (ii) $1 + x, -y, 1/2 + z$; (iii) $1/2 + x, y - 1/2, z$; (iv) $x, -y, z - 1/2$; (v) $x, -y, 1/2 + z$; (vi) $x - 1, -y, z - 1/2$.

lengths, bond angles, and anisotropic thermal parameters are given in Tables SII–SVI.

Magnetic Measurements. These were carried out with four instruments, namely: (i) a Faraday-type magnetometer working in the 4–300 K temperature range; (ii) a low-field SQUID magnetometer working below 40 K with magnetic fields on the order of 1 Oe; (iii) a high-field SQUID magnetometer working with magnetic fields up to 80 kOe; (iv) the very-high-field water-cooled magnetometer working up to 200 kOe of the Service National des Champs Intenses in Grenoble, France. All the instruments except the first one work down to 1.7 K.

EPR Measurements. The X-band powder EPR spectra were recorded at various temperatures between 4.2 and 300 K with an ER 200D Bruker spectrometer, equipped with a helium continuous-flow cryostat, a Hall probe, and a frequency meter.

Description of the Structure

The crystal structure of $(rad)_2Mn_2[Cu(opba)]_3(DMSO)_2 \cdot 2H_2O$ has been briefly described in ref 30, but due to the lack of space many details and subtleties of this structure were not reported. The general architecture is the following: There are two equivalent two-dimensional networks, noted A and B. Each network consists of parallel honeycomb layers. A layer is made up of edge-sharing hexagons with a Mn(II) ion at each corner and a Cu(II) ion at the middle of each edge. Two nearest neighbor metal ions are bridged by an oxamato group. The mean length of an edge is 10.797(5) Å, and the mean separation between opposite corners is 21.519(6) Å. These layers stack above each other in a graphite-like fashion: each manganese atom of a layer projects at the

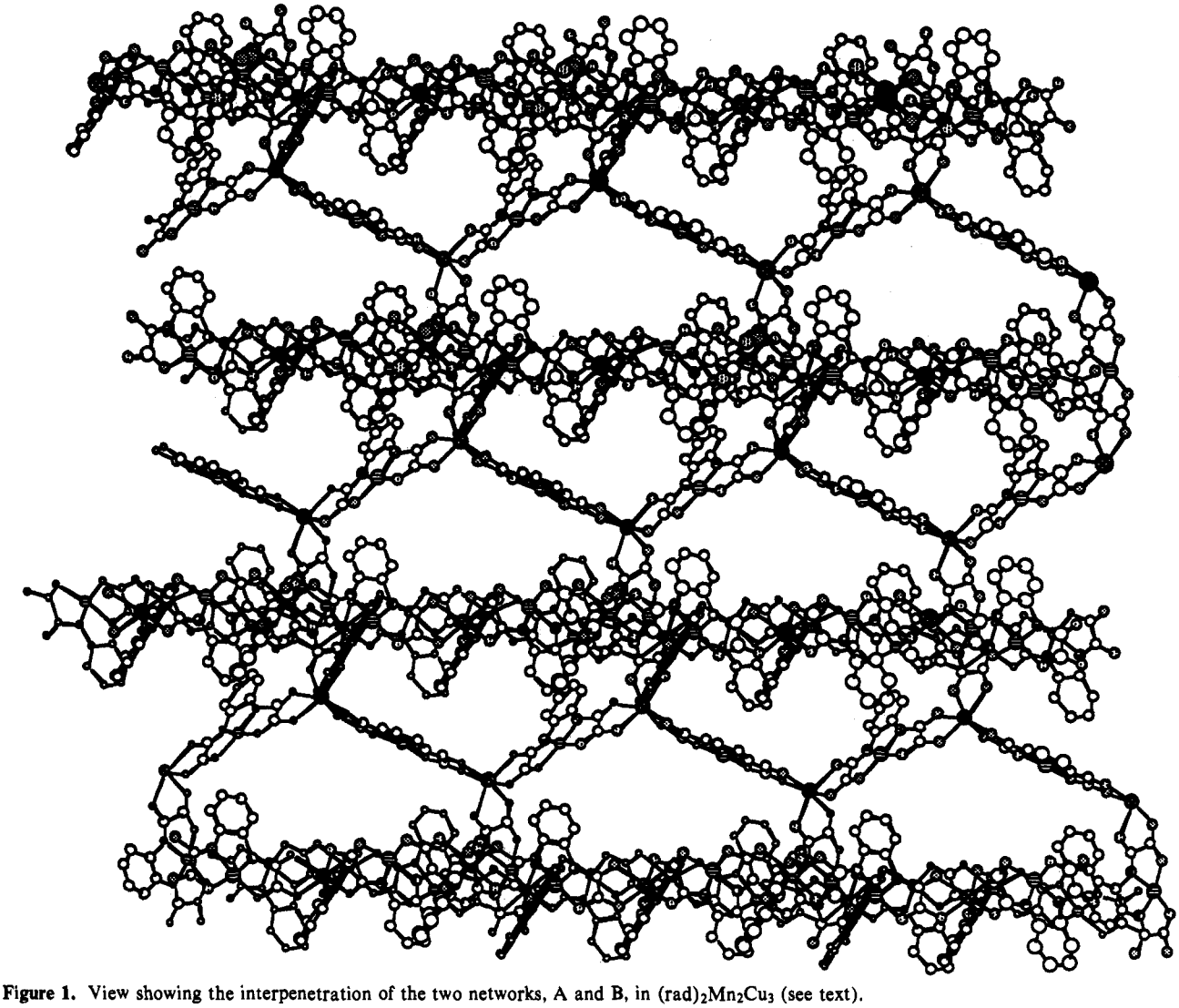

Figure 1. View showing the interpenetration of the two networks, A and B, in $(rad)_2Mn_2Cu_3$ (see text).

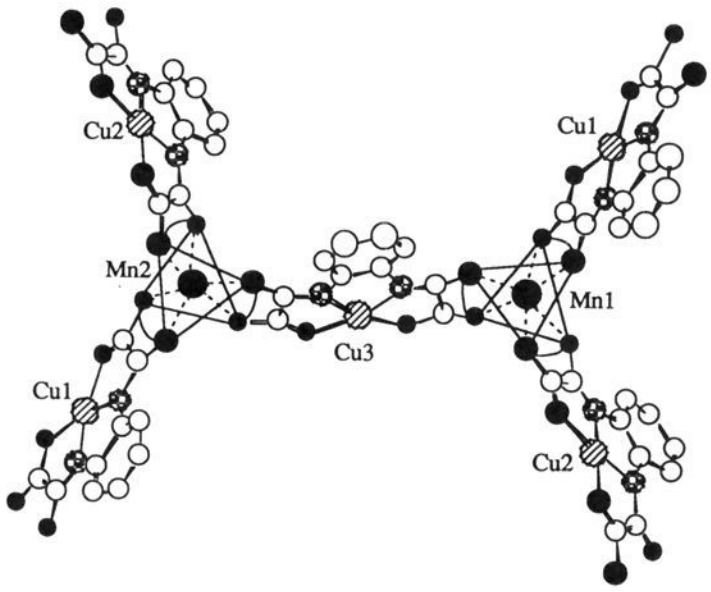

Figure 2. View showing the coordination spheres of two manganese atoms, Mn1 and Mn2, occupying two adjacent corners of a hexagon in $(rad)_2Mn_2Cu_3$.

center of hexagons belonging to the two adjacent layers. The mean interlayer separation is equal to 14.8 Å.

One of the main original features of the structure is the way the A and B networks are connected. These networks make a dihedral angle of 83.4° and interpenetrate each other with a full interlocking of the hexagons, as shown in Figure 1. In this figure, where for the sake of clarity the radical cations as well as the solvent molecules were omitted, a layer of one of the networks, say A, lies parallel to the sheet, and four layers of the network B are nearly perpendicular to this sheet. A Cu(II) ion of a hexagon B is located very nearby the center of a hexagon A, and vice versa. The topology is that of a three-dimensional wire netting. The networks A and B are connected further through the radical cations, as we will discuss below.

Let us now describe the surroundings of the metal centers. The manganese atom is bonded to six oxygen atoms arising from three oxamato groups, the average value of the Mn–O bond lengths being equal to 2.20(2) Å. The three copper atoms bridged to a manganese atom through oxamato groups are crystallographically independent (vide infra). In such surroundings the manganese atom occupies a chiral site. The structure presents a perfect alternation of Λ and Δ chiral sites, noted Mn1 and Mn2, as shown in Figure 2. However, these Mn1 and Mn2 sites are not strictly related through a mirror plane, so that it would not be correct to speak about a racemic composition.

Each copper atom has a 4 + 2 coordination with two nitrogen and two oxygen atoms arising from two oxamato groups in the basal plane, and two oxygen atoms arising from either DMSO molecules or rad^+ cations in the apical positions. The average values of the Cu–N and Cu–O basal bond lengths are equal to 1.94(2) and 1.98(2) Å, respectively. Actually, there are three crystallographically independent copper atoms, noted Cu1, Cu2, and Cu3, as shown in Figure 3. Cu1 is bonded to two DMSO molecules with Cu1–O(DMSO) apical bond lengths equal to 2.55(6) and 2.57(5) Å. Both Cu2 and Cu3 are bonded to two rad^+ groups with Cu2–O(rad^+) bond lengths of 2.90(2) and 2.94(2) Å and Cu3–O(rad^+) bond lengths of 2.82(1) and 3.01(2) Å.

Let us now focus on the structural details of a hexagon. Figure 4 represents such an hexagon belonging to the network A. It shows an alternation of the Mn1 and Mn2 chiral sites as well as of the Cu1, Cu2, and Cu3 sites. Two crystallographically equivalent copper sites are opposite to each other in the hexagon. Nearby the center of a hexagon A, one can see a $Cu3_B$ site belonging to a hexagon B. Cu_3B is bonded to two rad^+ cations with $Cu3_B$–O(rad^+) apical bonds, each rad^+ cation belonging also to the coordination sphere of a $Cu2_A$ site. In other words the rad^+ cations play the role of bridging ligands between $Cu2_A$ and $Cu3_B$ sites, affording $Cu2_A$–rad–$Cu3_B$–rad chains. Similarly, each $Cu3_A$ site is located nearby the center of a hexagon B and

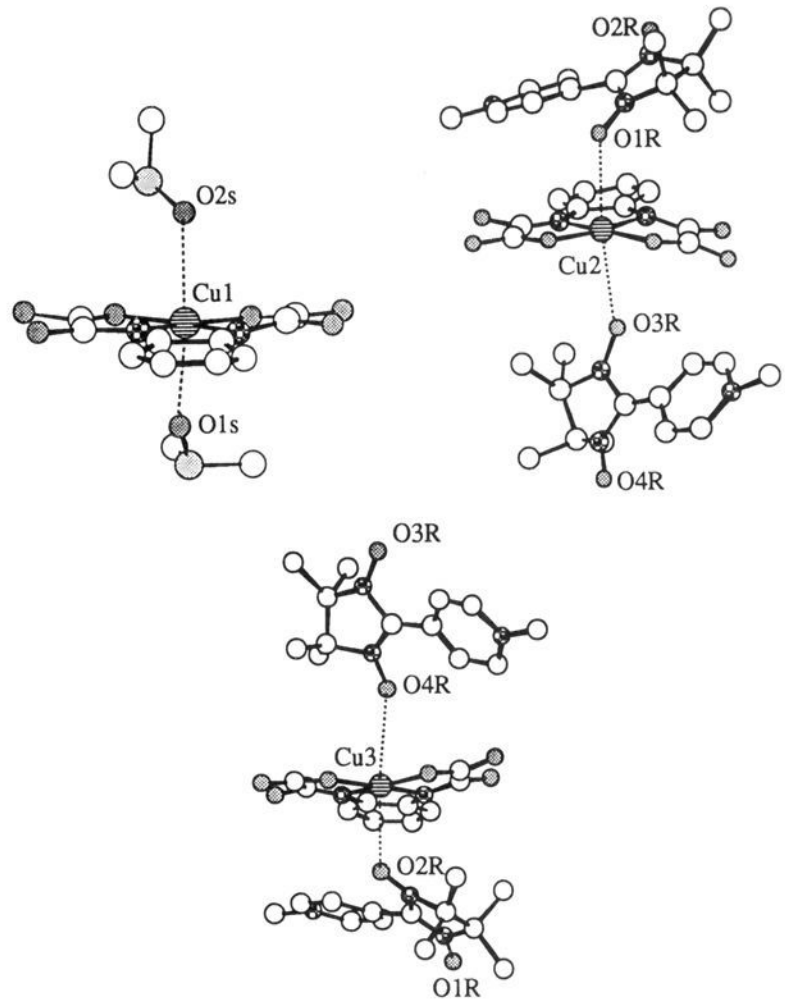

Figure 3. View showing the coordination spheres of the three crystallographically nonequivalent copper atoms in $(rad)_2Mn_2Cu_3$.

is connected to two Cu_2B sites through the rad^+ cations, which affords $Cu3_A$–rad–$Cu2_B$–rad chains. These chains run along the [112] and [1$\bar{1}$2] directions, respectively. These directions make an angle of 83.4°. The two $Cu2_A$---$Cu3_B$ (or $Cu3_A$---$Cu2_B$) intrachain separations are equal to 10.612(5) and 8.700(5) Å, respectively.

There are two crystallographically independent rad^+ units. Within each radical cation the two N–O groups and the sp^2 carbon atom of the five-membered ring are almost coplanar. The dihedral angle between this mean plane and the plane of the pyridinium ring is equal to 25.6° for one of the radical cations and 30.6° for the other.

The water molecules present in the structure are noncoordinated; they are located in the tunnels limited by the interlocked perpendicular layers.

Magnetic Properties

We will successfully study the temperature dependence of the magnetic susceptibility, the temperature dependence of the magnetization, and the field dependence of the magnetization.

Temperature Dependence of the Magnetic Susceptibility. The magnetic susceptibility data are shown in Figure 5 in the form of the $\chi_M T$ versus T plot, χ_M being the molar magnetic susceptibility and T the temperature. At room temperature $\chi_M T$ is equal to 8.60 cm^3 K mol^{-1}, which is lower than expected for two Mn(II), three Cu(II), and two organic radical isolated spin carriers. As T is lowered, $\chi_M T$ first decreases, reaches a minimum around 115 K ($\chi_M T$ = 7.77 cm^3 K mol^{-1}), and then increases more and more rapidly. Below ca. 25 K, $\chi_M T$ reaches very high values and becomes strongly field dependent. This $\chi_M T$ versus T profile is characteristic of ferrimagnetic behavior with a three-dimensional magnetic ordering below ca. 25 K. It is actually rather similar to that observed for $(NBu_4)_2Mn_2Cu_3$ with the minimum of $\chi_M T$ occurring almost at the same temperature. The presence of an additional spin carrier, the radical cation, does not modify significantly the curve. At any temperature down to ca. 30 K, one has roughly $\chi_M T$ for $(rad)_2Mn_2Cu_3$ = $\chi_M T$ for $(NBu_4)_2Mn_2Cu_3$ + 0.30 (in cm^3 K mol^{-1}).

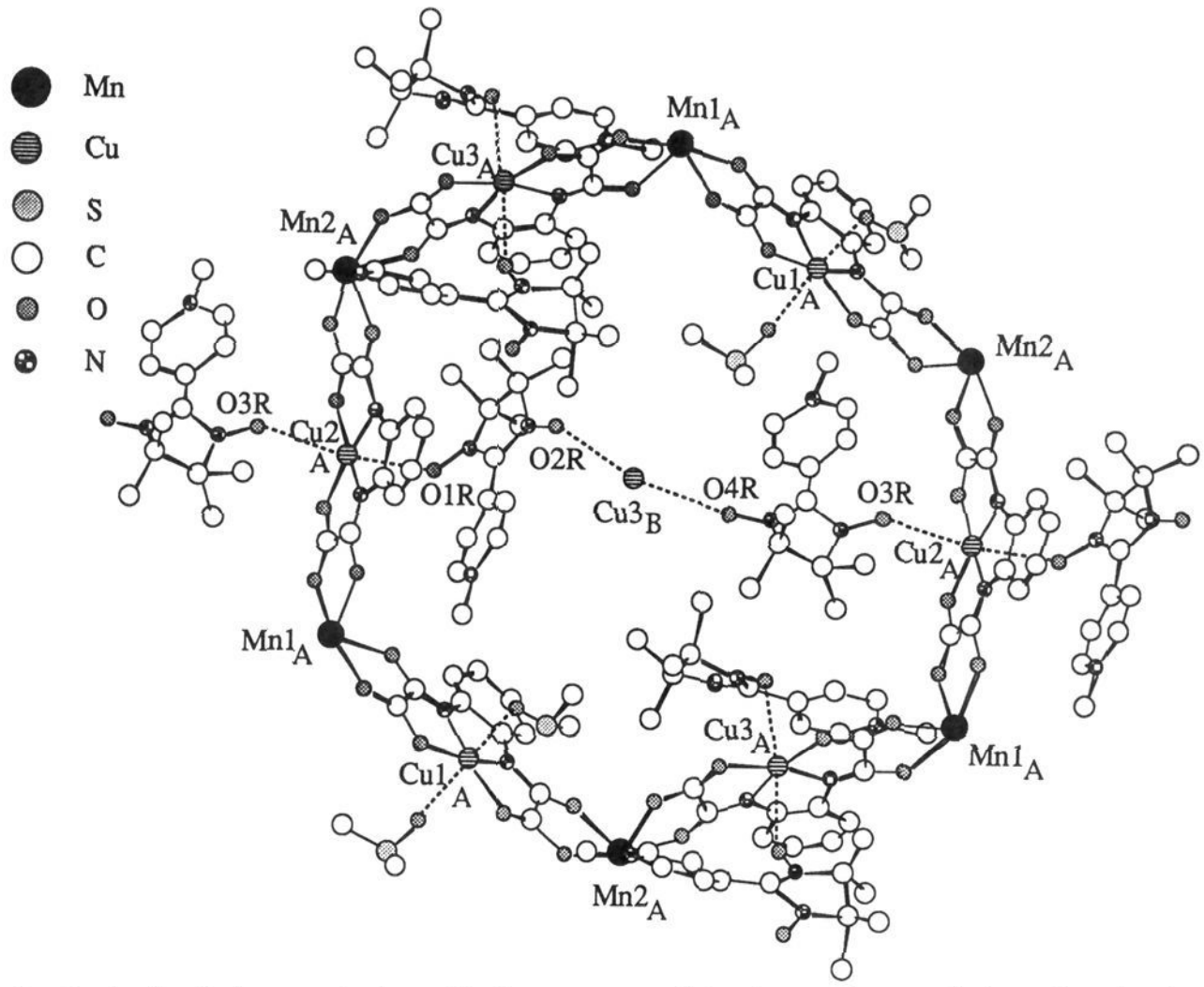

Figure 4. View showing the details of a hexagon A along with the copper atom belonging to a hexagon B, located nearby the center of the hexagon A in $(rad)_2Mn_2Cu_3$. This view emphasizes the presence of $Cu2_A$–rad–$Cu3_B$–rad chains connecting the A and B networks.

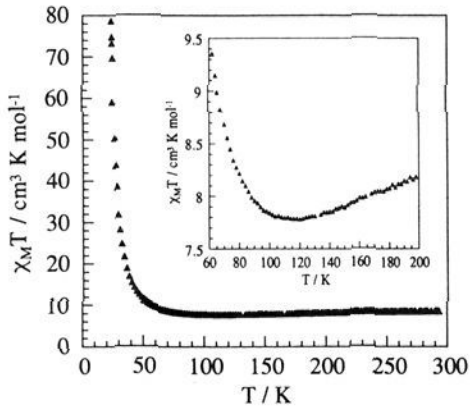

Figure 5. $\chi_M T$ versus T plot for $(rad)_2Mn_2Cu_3$. The inset emphasizes the minimum of $\chi_M T$ around 115 K.

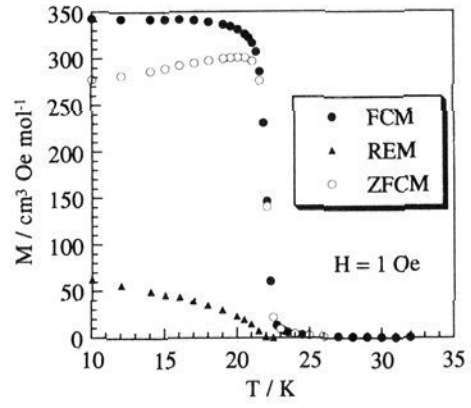

Figure 6. Magnetization M versus T curves for $(rad)_2Mn_2Cu_3$.

We did not attempt to interpret quantitatively the $\chi_M T$ versus T curve. Owing to the topology of the compound as well as the presence of three different spin carriers, deriving a theoretical expression of the magnetic susceptibility is probably an insurmountable task. The ferrimagnetic behavior with the decrease of $\chi_M T$ down to 115 K confirms the antiferromagnetic nature of the interaction between Mn(II) and Cu(II) ions through the oxamato bridge. On the other hand the magnetic susceptibility data do not provide any information on the role of the radical cations as far as the magnetic properties are concerned.

Temperature Dependence of the Magnetization. The magnetization versus temperature curves at a field of 1 Oe shown in Figure 6 were already discussed in ref 30. The field-cooled magnetization (FCM) measured upon cooling within the field shows a rapid increase of M below T_c = 22.5 K. The zero-field-cooled magnetization (ZFCM) measured upon cooling down to 5 K in zero field and then warming up within the field is lower than the FCM below T_c. Finally, when the sample is cooled down within the field and then warmed up in zero field, a remnant magnetization (REM) is observed, which vanishes at T_c. All of these features are now well documented.[35] They are characteristic of a magnetically ordered state below T_c = 22.5 K.

Field Dependence of the Magnetization. The field dependence of the magnetization at 10 K up to 60 kOe has been presented in ref 30. The $M = f(H)$ curve revealed a rather peculiar behavior. As expected for a magnet, the zero-field susceptibility, $(\partial M/\partial H)_{H=0}$, is extremely large, and a magnetization of about 4 Nβ (Bohr magneton per mole) is obtained within a few tens of oersteds. As the field is increased further, instead of showing a saturation, M increases smoothly and reaches a value of 4.9 Nβ at 60 kOe. To get more information on the magnetic structure of our compound, we reinvestigated the magnetization at 4.2 K up to 200 kOe. The new curve is shown in Figure 7. Again, a magnetization of about 4.2 Nβ is obtained within a very low field; then M increases as H increases and eventually is equal to 6.5 Nβ at 200 kOe. Even with such a very high field, the saturation is not reached. Above ca. 80 kOe the M versus H plot is roughly linear.

To begin the discussion of these magnetization data, it is interesting to compare the $M = f(H)$ curves for $(rad)_2Mn_2Cu_3$ and $(NBu_4)_2Mn_2Cu_3$. The two curves are very different; for any value of the field, the former is lower than the latter. Indeed, the magnetization for $(NBu_4)_2Mn_2Cu_3$ rapidly reaches a saturation

(33) *International Tables for X-ray Crystallography*; Kynoch Press: Birmingham, U.K., 1974; Vol. IV.

(34) Molen (Molecular Structure Enraf-Nonius); Enraf-Nonius: Delft, The Netherlands, 1990.

(35) Hitzfeld, M.; Ziemann, P.; Buckel, W.; Claus, H. *Phys. Rev. B* **1984**, *29*, 5023.

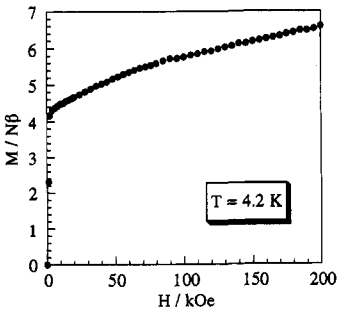

Figure 7. Field dependence of the magnetization for $(rad)_2Mn_2Cu_3$ at 4.2 K up to 200 kOe.

value of 7.1 Nβ, which agrees with what is anticipated for all the Mn(II) local spins aligned along the field direction and the Cu(II) local spins along the opposite direction.[29] The difference between the two curves is clearly related to the presence of the rad^+ cations in $(rad)_2Mn_2Cu_3$.

We have seen that the magnetic susceptibility data do not provide any information as for the preferred spin orientation of the rad^+ cations with regard to the orientations of the Mn(II) and Cu(II) spins. Let us examine to what extent this kind of information may be deduced from the magnetization data. Three situations in principle are possible:

(i) The rad^+ spins do not interact with the Mn(II) and Cu(II) spins. If this is so, the magnetization is the sum of two terms, namely $M(Mn_2Cu_3)$ for the $Mn_2[Cu(opba)]_3$ core and $M(rad^+)$ for the two radical cations. The $M(Mn_2Cu_3)$ curve should be close to that measured for $(NBu_4)_2Mn_2Cu_3$, and the $M(rad^+)$ curve would be the Brillouin function for two noninteracting local spin doublets. It follows that in this hypothesis the $M = f(H)$ curve for $(rad)_2Mn_2Cu_3$ should be above that for $(NBu_4)_2Mn_2Cu_3$ with a saturation value of about 9 Nβ, which is clearly not the case.

(ii) The rad^+ spins are antiferromagnetically coupled with the Cu(II) spins. If this is so, not only should the $M = f(H)$ curve for $(rad)_2Mn_2Cu_3$ be again above that for $(NBu_4)_2Mn_2Cu_3$ but the saturation value of 9 Nβ would also be more rapidly reached. This hypothesis can be ruled out.

(iii) The rad^+ spins tend to align parallel with the Cu(II) spins (i.e. antiparallel with the Mn(II) spins). In such a case the profile of the magnetization curve will depend on the magnitude of the rad^+–Cu(II) ferromagnetic interaction (and/or the magnitude of the rad^+–Mn(II) antiferromagnetic interaction). If this type of coupling between the rad^+ cations and the metal ions is very large, then a rapid saturation of about 5 Nβ should be reached (in fact the saturation magnetization should be slightly weaker than 5 Nβ due to the fact that the g-factor for the Cu(II) ion is larger than 2.00). If, on the other hand, the rad^+–Cu(II) ferromagnetic interaction (and/or the rad^+–Mn(II) antiferromagnetic interaction) is weak enough, a magnetization slightly lower than 5 Nβ will be rapidly reached. When the field increases further, a decoupling between the rad^+ and Cu(II) spins will occur, and the magnetization will progressively increase. A high-field limit for M of about 9 Nβ is expected, corresponding to the field range where the rad^+–Cu(II) interactions are overcome. Figure 7 unambiguously indicates that we are in such a situation.

An alternative interpretation for the $M = f(H)$ curve might be considered. The networks A and B are nearly perpendicular to each other. For each of the two ferrimagnetic networks, in the absence of local anisotropy, the preferred spin orientation is expected to be perpendicular to the layers, which corresponds to the best compromise between dipolar and exchange interactions.[36] In $(rad)_2Mn_2Cu_3$ the local anisotropy of the three spin carriers is, indeed, very weak. It follows that the preferred spin orientations of A and B are roughly orthogonal, and increasing the field results in a progressive alignment of the A and B layer spins and hence in an increase of the magnetization. This effect, however, should be very small. Indeed, the dipolar interactions are weak, so that the magnetic anisotropy for A and B should be weak as well. Therefore, it does not make any sense to imagine that a field of 200 kOe is not sufficient to align parallel the layer spins.

The fact that $(rad)_2Mn_2Cu_3$ presents a weak magnetic anisotropy is confirmed by the narrowness of the hysteresis loop. At 4.2 K the coercive field is less than 10 Oe. We will come back to this point in the discussion.

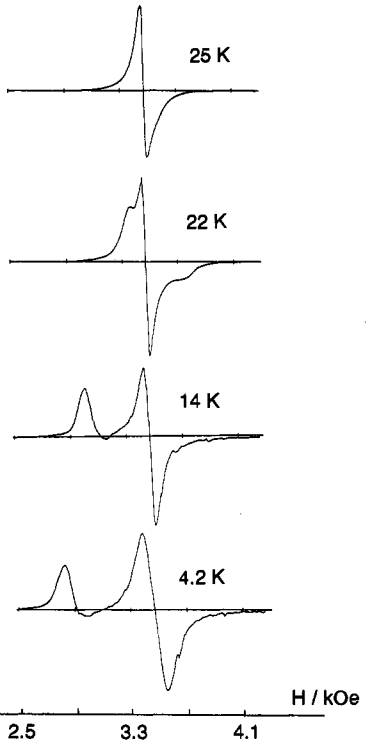

Figure 8. X-band powder EPR spectra of $(rad)_2Mn_2Cu_3$ at various temperatures above and below T_c = 22.5 K.

EPR Properties

The X-band powder EPR spectrum of $(rad)_2Mn_2Cu_3$ at room temperature shows a single and symmetrical resonance centered at g = 1.995. The line width is equal to 55 Oe. As the temperature is lowered down to T_c = 22.5 K, two slight modifications are observed, namely: (i) The resonance is shifted toward the high fields. For instance, it is centered at g = 1.983 at 120 K and at 1.955 at 25 K. This g-shift might be due both to short-range effect and to the fact that, on decreasing temperature, states corresponding to opposite spins on Mn(II) and Cu(II) are selectively populated.[38] (ii) This resonance becomes less symmetrical. On the other hand, there is no variation in the line width. The spectra above T_c are rather similar to those observed with the other Mn(II)Cu(II) magnets. The line width for $(rad)_2Mn_2Cu_3$, however, is the weakest found so far,[9-11,29,37] which clearly indicates that the magnetic behavior is dominated by the exchange interaction effect.[38]

At T_c and below, the spectrum is deeply modified, as shown in Figure 8. The resonance at g = 1.955 is still present, but new features appear at lower and higher fields. One of them is very intense and strongly temperature dependent; this new feature appears as a low-field shoulder of the main resonance at T_c and is shifted toward the low fields as T decreases. It is located around

(36) Caneschi, A.; Gatteschi, D.; Sessoli, R. In *Magnetic Molecular Materials*; Gatteschi, D., Kahn, O., Miller, J. S., Palacio, F., Eds.; Kluwer: Dordrecht, The Netherlands, 1991; p 215.

(37) Gatteschi, D.; Guillou, O.; Zanchini, C.; Sessoli, R.; Kahn, O.; Verdaguer, M.; Pei, Y. *Inorg. Chem.* **1989**, *28*, 287.

(38) Bencini, A.; Gatteschi, D. *EPR of Exchange Coupled Systems*; Springer-Verlag: Berlin, 1990.

3000 Oe at 15 K and around 2800 Oe at 4.2 K. This modification of the spectrum in the magnetically ordered state is due to the ferromagnetic resonance phenomenon.[39-41] We cannot provide a full interpretation of the spectra yet. We need to investigate other systems. However, we would like to suggest a very simple qualitative picture of the phenomenon.

Above T_c the system may be schematically described as consisting of paramagnetic centers resonating at $g = 1.95$, i.e. with an applied magnetic field $H°$. At T_c and below, the field experienced by each magnetic center is[42-44]

$$H = H_{ext} + H_{loc} \quad (1)$$

where H_{ext} is the external applied field and H_{loc} is the local field in the magnetically ordered state. At given external field and temperature, H_{loc} may be approximated by

$$H_{loc} = H_{loc}° + H_d \quad (2)$$

$H_{loc}°$ is the field induced by the external field, directed along the same direction as H_{ext}, and H_d is the demagnetizing field which tends to oppose $H_{loc}°$. While $H_{loc}°$ at given external field and temperature depends on the chemical nature of the compound, H_d also depends on structural factors related to the morphology of the grains in the sample. For a spherical grain $H_{loc}°$ and H_d exactly compensate each other, and the local field is zero. On the other hand, for a needle-shaped grain H_d is minimum, and H_{loc} takes the maximum value $H_{loc}°$. In a powder sample with randomly shaped grains H_{loc} may take all values from zero to $H_{loc}°$ and the resonance is realized not for a unique value H_0 of the field but for a field range from $H°-H_{loc}°$ to $H°$. Each spectrum below T_c in Figure 8 (which is the derivative of the absorption curve) corresponds to such an absorption covering a large field range. This picture is obviously oversimplified; it is however consistent with the temperature dependence of the low-field feature. As a matter of fact, for a given value (not too large) of the applied field, the magnetization, and therefore $H_{loc}°$, increases as the temperature is lowered. It follows that $H°-H_{loc}°$ decreases as T decreases. The absorption begins at a lower external field, which is observed in the spectra.

Discussion

In this section we would like to discuss further three aspects of our findings, namely the unique structure of the compound, then the role of the radical cation as far as the magnetic properties are concerned, and finally the quasi absence of coercivity.

Our starting idea when replacing an innocent cation like *N*-tetrabutylammonium by a nitronyl nitroxide cation was to connect the Mn_2Cu_3 layers and therefore to increase the magnetic dimensionality of the material. It is indeed well established that the nitronyl nitroxide radicals can bridge metal ions through the two N–O groups.[21,22] The neutral nitronyl nitroxides, however, are weak bases and link metal ions only when these ions are made electron-attractive, for instance with (hexafluoroacetyl)acetonato ligands.[22] Since the copper(II) precursor is anionic, we thought that using a nitronyl nitroxide cation could favor the rad–Cu interaction. What actually happened is that the size of the Mn_6Cu_6 hexagon nicely fits the presence of two nitronyl nitroxide units and a Cu(II) ion belonging to another layer, affording Cu(II)–rad$^+$ chains. In other terms the key factors favoring the interlocking of the two networks are (i) the electrostatic interactions between negative Cu(II)-containing units and positive radicals; (ii) the size of the radical as compared to the size of the hexagonal cavity; (iii) the bridging ability of the nitronyl nitroxide. The fact that rad$^+$ carries a $^1/_2$ spin does not seem to play a role in the interlocking.

$(rad)_2Mn_2Cu_3$ is one of the very few two- or three-dimensional molecular structures presenting a complete interlocking of independent infinite networks. Other examples are silver tricyanomethide,[45] trimesic acid,[46] diaquabis(4,4′-bipyridine)zinc hexafluorosilicate,[47] and zinc bis(tricyanomethide).[48] Interlocking of rings in discrete supramolecular units is also an area of research which has known beautiful developments in the last few years.[49] The best documented examples are probably the catenanes resulting from the interlocking of molecular threads.[50] Both Sauvage's and Stoddart's groups have contributed to this area in quite a successful manner.[51-54]

From a magnetic point of view, what is crucial for $(rad)_2Mn_2Cu_3$ is the role of the radical cation. The magnetization measurements have revealed that in zero field the rad$^+$ spins tend to align parallel to the Cu(II) spins, hence antiparallel to the Mn(II) spins. When the field increases, a progressive alignment of the rad$^+$ spins along the field direction occurs.

Gatteschi and co-workers already showed that the interaction between a Cu(II) ion and a nitronyl nitroxide radical occupying an apical position may be ferromagnetic.[22] This behavior was attributed to the orthogonality of the copper $d_{x^2-y^2}$-type and radical p_π-type magnetic orbitals.[25,55] However, in Gatteschi's examples such a ferromagnetic interaction was detected when the Cu–O(radical) apical bond length is on the order of 2.4 Å, whereas in $(rad)_2Mn_2Cu_3$ those distances are on the order of 2.9 Å. Perhaps in our case the preferred spin orientation of the rad$^+$ cations is determined not only by rad$^+$–Cu(II) ferromagnetic interactions but also by the rad$^+$–Mn(II) antiferromagnetic interactions. Indeed, each oxygen atom of a rad$^+$ unit not only is weakly bonded to a copper atom but also is rather close to two manganese atoms, the corresponding Mn–O(rad$^+$) distances ranging from 5.31 to 6.64 Å. Even if Mn–O(rad$^+$) is larger than Cu–O(rad$^+$), the relative orientation of the magnetic orbitals between Mn(II) and rad$^+$ is favorable to provide some through-space antiferromagnetic interaction.

Let us try to estimate the magnitude of the interaction between a rad$^+$ unit and the Mn_2Cu_3 core from the $M = f(H)$ curve of Figure 7. For that let H_c define the field necessary to overcome the antiferromagnetic interaction between the radical cation and the metal core. Assuming that the compound is magnetically isotropic, in the mean-field approximation the saturation magnetization is reached when the field is equal to $2H_c$.[42-44,56,57] In the field range (above ca. 80 kOe) where M varies linearly with H, the magnetization may be written as

(39) Kittel, C. *Phys. Rev.* **1948**, *73*, 155.
(40) Phaff, A. C.; Swüste, C. H. W.; de Jonge, W. J. M.; Hoogerbeets, R.; van Duyneveldt, *J. Phys. C* **1984**, *17*, 2583.
(41) Hoogerbeets, R.; van Duyneveldt, A. J.; Phaff, A. C.; Swüste, C. H. W.; de Jonge, W. J. M. *J. Phys. C* **1984**, *17*, 2595.
(42) Morrish, A. H. *The Physical Principles of Magnetism*; Krieger: New York, 1980.
(43) Herpin, A. *Théorie du Magnétisme*; P.U.F.: Paris, 1968.
(44) Martin, D. H. *Magnetism in Solids*; MIT Press: Cambridge, MA, 1967.
(45) Konnert, J.; Britton, D. *Inorg. Chem.* **1966**, *7*, 1193.
(46) Duchamp, D. J.; Marsh, R. E. *Acta Crystallogr., Sect. B* **1969**, *25*, 5.
(47) Gable, R. W.; Hoskins, B. F.; Robson, R. *J. Chem. Soc., Chem. Commun.* **1990**, 1677.
(48) Batten, S. R.; Hoskins, B. F.; Robson, R. *J. Chem. Soc., Chem. Commun.* **1991**, 445.
(49) Sauvage, J. P., Ed. Topology in Chemistry. *New J. Chem.* **1993**, *7*, 613–764.
(50) Schill, G. *Catenanes, Rotaxanes, and Knots*; Academic Press: New York, 1971.
(51) Sauvage, J. P. *Acc. Chem. Res.* **1990**, *23*, 319.
(52) Dietrich-Buchecker, C. O.; Sauvage, J. P. In *Bioorganic Frontiers*; Degas, H., Ed.; Springer-Verlag: New York, 1991; Vol. 2.
(53) Ortholand, J. Y.; Slawin, A. M. Z.; Spencer, N.; Stoddard, J. F.; Williams, D. J. *Angew. Chem., Int. Ed. Engl.* **1989**, *28*, 1394.
(54) Anelli, P. L.; Ashton, P. R.; Ballardini, R.; Balzani, V.; Delgado, M.; Gandolfi, M. T.; Goonow, T. T.; Kaifer, A. E.; Philp, D.; Pietraszkiewicz, M.; Prodi, L.; Reddington, M. V.; Slawin, A. M.; Spencer, N.; Stoddart, J. F.; Vicent, C.; Williams, D. J. *J. Am. Chem. Soc.* **1992**, *114*, 193.
(55) Caneschi, A.; Gatteschi, D.; Grand, A.; Laugier, J.; Rey, P.; Pardi, L. *Inorg. Chem.* **1988**, *27*, 1031.
(56) Stryjewski, E.; Giordano, N. *Adv. Phys.* **1977**, *26*, 487.
(57) Carlin, R. L. *Magnetochemistry*; Springer-Verlag: Berlin, 1986.

$$M = M_s(Mn_2Cu_3) + 2[M_s(rad^+)](H/H_c - 1) \quad (3)$$

so that, when H is equal to $2H_c$, M reaches the saturation. $M_s(Mn_2Cu_3)$ and $M_s(rad^+)$ in eq 3 stand for the components of the saturation magnetization arising from the metal core and the radical cations, respectively. Equation 3 can be rewritten as

$$M = [(5g_{Mn} - 3g_{Cu}/2) + 2g_{rad}(H/H_c - 1)]\ N\beta \quad (4)$$

where g_{Mn}, g_{Cu}, and g_{rad} are the local g-factors. Taking $g_{Mn} = g_{rad} = 2$ and fitting the linear range of the $M = f(H)$ curve with eq 4 result in $H_c = 247.5$ kOe with $g_{Cu} = 2.07$. This critical field, H_c, is related to the magnitude of the interaction between the radical cation (with the spin quantum number S_{rad}) and the metallic core through[41-43,55]

$$\beta g_{rad} S_{rad} H_c = \sum_i |a_i J_i| \quad (5)$$

where the summation runs on all the M_i nearest neighbor metal ions interacting with a rad$^+$ unit and $|a_iJ_i|$ is the energy cost to break a rad$^+$–M_i interaction.

If the interaction of rad$^+$ with the metal core is assumed to be entirely due to the rad$^+$–Cu(II) interactions along the chains, then a is equal to 1. Indeed, the singlet–triplet energy gap resulting from the coupling of two $^1/_2$ local spins is equal to J. It follows that the sum of the two rad$^+$–Cu(II) interaction parameters, $J_{radCu,1} + J_{radCu,2}$, is equal to 23 cm^{-1}. The plus sign means that the interaction is ferromagnetic. It is amazing to realize that in this case the magnetic field destroys a *ferromagnetic* interaction! A rather similar behavior was reported for a Mn(II)–radical compound.[58]

It is also possible to assume that the radical cation–metal core interaction is due to the antiferromagnetic coupling of rad$^+$ with the four nearest neighbor Mn(II) ions. If this is so, eq 5 must be applied with $a = 3$. Indeed, the quintet–septet energy gap resulting from the coupling of $S_{Mn} = ^5/_2$ and $S_{rad} = ^1/_2$ local spins is equal to 3 J. In that case, one obtains $\sum_i J_{radMn,i} = -7.6$ cm^{-1}, the minus sign pointing out that the interaction is now antiferromagnetic.

Of course, the two kinds of interactions may be involved, so that we can write a relation of the form

$$\sum_{i=1,2} J_{radCu,i} + 3\sum_{i=1-4} |J_{radMn,i}| = 23\ cm^{-1} \quad (6)$$

the $J_{radCu,i}$ parameters being positive and the $J_{radMn,i}$ parameters being negative. According to the structure, particularly the M–O(rad$^+$) distances, the first term in the left-hand side of eq 6 probably dominates.

At this stage it is interesting to take a look at the magnetic properties of (rad)$_2$[Cu(opba)]·H$_2$O. $\chi_M T$ for this compound increases as T is lowered, which is in line with a spin-quartet ground state resulting from rad$^+$–Cu(II) ferromagnetic interactions. The magnetic data can be fairly well fitted with a model of three spin carriers rad$^+$–Cu(II)–rad$^+$. Neglecting the interaction between the symmetrically related terminal rad$^+$ units results in $J_{rad\,Cu} = 5.6$ cm^{-1} (with $g_{rad} = 2.00$ and $g_{Cu} = 2.07$). Unfortunately we do not know the crystal structure of (rad)$_2$[Cu(opba)]·H$_2$O yet. In particular we ignore the Cu–O(rad$^+$) bond lengths.

What is surprising and actually a bit disappointing in the magnetic properties of (rad)$_2$Mn$_2$Cu$_3$ is that, despite the three-dimensional character, the critical temperature ($T_c = 22.5$ K) is still rather low. T_c for (rad)$_2$Mn$_2$Cu$_3$ is not much higher than that for (NBu$_4$)$_2$Mn$_2$Cu$_3$ ($T_c = 15$ K). At first view there is a sort of contradiction between the T_c value and the fact that the rad$^+$ units couple magnetically the A and B networks. A first explanation is that in zero field the rad$^+$ spins tend to align antiparallel to the Mn$_2$Cu$_3$ spins; the ground-state spins for (rad)$_2$Mn$_2$Cu$_3$ and (NBu$_4$)$_2$Mn$_2$Cu$_3$ are $^5/_2$ and $^7/_2$, respectively, and T_c depends not only on the magnitude of the interactions between the spin carriers but also on the magnitude of the interacting spins. In other respects, and this might well be the main reason of the rather low T_c value, the rad$^+$–Cu(II) chains connecting the A and B networks are not regular in the sense where the rad$^+$–Cu(II) interactions are not all equivalent. A careful examination of the structural details indicates that each rad$^+$ unit is a bit more efficiently linked to one of the nearest neighbor Cu(II) ions than to the other, which obviously diminishes the three-dimensional character. Similarly, a Cu(II) ion belonging to network A is not exactly at the center of a hexagon B, the Cu_A---Cu_B separations ranging from 8.214 to 10.356 Å, which decreases further the three-dimensional character. It is also worthwhile to notice that in a Cu_A–rad$^+$–Cu_B linkage the Cu_A and Cu_B atoms are not located within the mean plane of the O–N–C–N–O nitronyl nitroxide group. For one of the radical cations the distances of the Cu2 and Cu3 atoms from this mean plane are −2.64 and 2.41 Å, respectively. For the other radical cation these distances are 1.05 and −1.15 Å, respectively. In other words, using the same topology, it might be possible to tilt the mean plane of the nitronyl nitroxide group in order to minimize the Cu–O apical bond lengths and consequently increase the rad$^+$–Cu(II) ferromagnetic interaction. This is, of course, a rather optimistic view. Nevertheless we are presently working along this line.

The last point we would like to discuss briefly deals with the magnetic hysteresis loop for (rad)$_2$Mn$_2$Cu$_3$. A magnet is characterized not only by its critical temperature but by its coercive field and remnant magnetization as well. In the case of (rad)$_2$Mn$_2$Cu$_3$ the coercive field is extremely weak, less than 10 Oe at 4.2 K. The coercivity of a magnet depends on both the chemical nature of the compound and structural factors like grain size and shape. As far as the chemical factors are concerned, the key parameter is the magnetic anisotropy of the spin carriers. In (rad)$_2$Mn$_2$Cu$_3$ the three spin carriers possess a very weak magnetic anisotropy. We recently observed that replacing Mn(II) by Co(II) results in a (rad)$_2$Co$_2$Cu$_3$ system exhibiting a coercive field at 1.7 K as large as 3 kOe.[26] This comparison between (rad)$_2$Mn$_2$Cu$_3$ and (rad)$_2$Co$_2$Cu$_3$ emphasizes the role of the local anisotropy in a spectacular fashion.

The coercive field for (rad)$_2$Mn$_2$Cu$_3$ is even weaker than that for (NBu$_4$)$_2$Mn$_2$Cu$_3$. This situation is probably related to the structural differences between the two compounds. In a Mn$_2$Cu$_3$ ferrimagnetic layered compound the preferred spin orientation is perpendicular to the layers.[36] When two layered networks are almost perpendicular to each other, as in (rad)$_2$Mn$_2$Cu$_3$, the preferred spin orientation is not along a direction any longer but along all the directions of a circle; the weak anisotropy of the Mn$_2$Cu$_3$ layer is even reduced in the interlocked system.

Conclusion

(rad)$_2$Mn$_2$Cu$_3$ is the first molecular-based magnet with a three-dimensional structure we succeeded in synthesizing. The three-dimensional character is achieved through quite an unusual way, by interpenetrating two nearly perpendicular layered networks. From both structural and magnetic points of view the connection between the two networks is realized by nitronyl nitroxide radical cations. The crystal structure as a whole seems to be one of great elegance and opens quite interesting perspectives in the field of tailor-made molecular materials.

The physical properties of the compound also present some novelties which deserve our attention. The Mn$_2$Cu$_3$ ferrimagnetic layers are magnetically coupled to each other by the radical cations. Those interact antiferromagnetically with the metal core. This interaction is rather weak and can be partially overcome by an external magnetic field. Probably the main origin of the rad$^+$–

(58) Caneschi, A.; Gatteschi, D.; Rey, D.; Sessoli, R. *Chem. Mater.* **1992**, *4*, 204.

metal core antiferromagnetic coupling is the ferromagnetic interaction between rad^+ cations and Cu(II) ions linked to each other in chains. The magnitude of this interaction was estimated from very-high-field magnetization measurements. Owing to the complexity of the system, no other magnetic (or spectroscopic) technique could provide this piece of information in a reliable way.

The EPR properties were also investigated in some detail, in particular in the magnetically ordered state, below $T_c = 22.5$ K. To the best of our knowledge, this ferromagnetic resonance study is one of the very first dealing with molecular-based magnets. We would like to incite the collegues working in this area to record the EPR spectra in the ferromagnetic state. The quantitative interpretation of these spectra is probably a very difficult task. Our feeling, however, is that a lot of original information can be obtained in that way.

The readers of this paper may be astonished that we do not say anything about the optical properties. This is due to the fact that the $\pi \rightarrow \pi^*$ transitions of the aromatic rings hide the Mn(II) spin-forbidden transitions characterizing these Mn(II)Cu(II) compounds.[59] We have at our disposal another Mn(II)Cu(II) magnet, ordering also at 22.5 K, which is more appropriate for optical studies.

In conclusion we would like to stress that the beauty of the structure and the originality of the magnetic properties of $(rad)_2Mn_2Cu_3$ push us to increase our endeavors in the field of molecular magnetism.

Supplementary Material Available: Ortep diagrams showing the three crystallographically independent Cu(opba) groups and the two crystallographically independent radical cations with the atom-labeling schemes (Figures S1 and S2) and tables of experimental crystallographic data, atomic coordinates, bond lengths, bond angles, and anisotropic thermal parameters (Tables SI–SVI) (15 pages); listing of observed and calculated structure factors (16 pages). This material is contained in many libraries on microfiche, immediately follows this article in the microfilm version of the journal, and can be ordered from the ACS; see any current masthead page for ordering information.

(59) Mathoniére, C.; Kahn, O.; Daran, J. C.; Hilbig, H.; Köhler, F. *Inorg. Chem.* **1993**, *32*, 4057.